

AD-A139 202

MODELING END-GAS KNOCK IN A RAPID-COMPRESSION MACHINE
(U) TRW ELECTRONICS AND DEFENSE SECTOR REDONDO BEACH CA
W B BUSH ET AL. 09 JAN 84 ARO-19972.1-EG

1/1

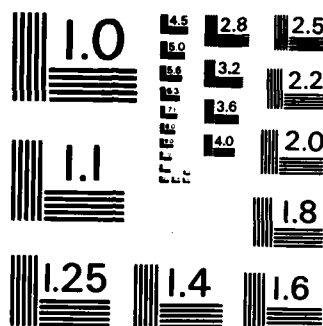
UNCLASSIFIED

DAGG29-83-C-0010

F/G 21/7

NL





MICROCOPY RESOLUTION TEST CHART
NATIONAL BUREAU OF STANDARDS-1963-A

SECURITY CLASSIFICATION OF THIS PAGE

REPORT DOCUMENTATION PAGE

1a. REPORT SECURITY CLASSIFICATION Unclassified		1b. RESTRICTIVE MARKINGS										
2a. SECURITY CLASSIFICATION AUTHORITY		3. DISTRIBUTION/AVAILABILITY OF REPORT Distribution unlimited										
2b. DECLASSIFICATION/DOWNGRADING SCHEDULE												
4. PERFORMING ORGANIZATION REPORT NUMBER(S)		5. MONITORING ORGANIZATION REPORT NUMBER(S)										
6a. NAME OF PERFORMING ORGANIZATION TRW Electronic & Defense Sector	6b. OFFICE SYMBOL (If applicable)	7a. NAME OF MONITORING ORGANIZATION U. S. Army Research Office										
6c. ADDRESS (City, State and ZIP Code) Redondo Beach, CA 90278		7b. ADDRESS (City, State and ZIP Code) Research Triangle Park, NC 27709										
8a. NAME OF FUNDING/SPONSORING ORGANIZATION	8b. OFFICE SYMBOL (If applicable)	9. PROCUREMENT INSTRUMENT IDENTIFICATION NUMBER DAAG29-83-C-0010										
8c. ADDRESS (City, State and ZIP Code)		10. SOURCE OF FUNDING NOS. <table border="1"><tr><td>PROGRAM ELEMENT NO.</td><td>PROJECT NO.</td><td>TASK NO.</td><td>WORK UNIT NO.</td></tr><tr><td></td><td></td><td></td><td></td></tr></table>		PROGRAM ELEMENT NO.	PROJECT NO.	TASK NO.	WORK UNIT NO.					
PROGRAM ELEMENT NO.	PROJECT NO.	TASK NO.	WORK UNIT NO.									
11. TITLE (Include Security Classification) Modeling End-Gas Knock in a Rapid-Compression Machine												
12. PERSONAL AUTHOR(S) W. B. Bush, F. E. Fendell, S. F. Fink												
13a. TYPE OF REPORT Reprint	13b. TIME COVERED FROM TO	14. DATE OF REPORT (Yr., Mo., Day) 1984 January 9	15. PAGE COUNT 16									
16. SUPPLEMENTARY NOTATION												
17. COSATI CODES <table border="1"><tr><td>FIELD</td><td>GROUP</td><td>SUB. GR.</td></tr><tr><td></td><td></td><td></td></tr><tr><td></td><td></td><td></td></tr></table>		FIELD	GROUP	SUB. GR.							18. SUBJECT TERMS (Continue on reverse if necessary and identify by block number) End-Gas Knock Premixed Combustion Explosion Rapid Compression Machine Flame Propagation	
FIELD	GROUP	SUB. GR.										
19. ABSTRACT (Continue on reverse if necessary and identify by block number) A rapid-compression machine is a laboratory apparatus to study aspects of the compression stroke, combustion event, and expansion stroke of an Otto cycle. As a simple model of such a machine, unsteady one-dimensional nonisobaric laminar flame propagation through a combustible premixture, enclosed in a variable volume, is examined in the asymptotic limit of Arrhenius activation temperature large relative to the conventional adiabatic flame temperature. In this limit, a thin propagating flame separates nondiffusive expanses of burned and unburned gas. The pressure through the enclosure is spatially homogeneous for smooth flame propagation. However, expansion of the hot burned gas results in compressional preheating of the remaining unburned gas, and in fact the spatially homogeneous gas may undergo autoconversion prior to arrival of the propagating flame. If such an explosion is too rapid for acoustic adjustment, large spatial differences in pressure arise and the resulting nonlinear waves produce audible knock. Here attention is concentrated on what fraction (if any) of the total charge may undergo autoconversion for a given operating (over)												
20. DISTRIBUTION/AVAILABILITY OF ABSTRACT DTIC FILE COPY UNCLASSIFIED/UNLIMITED SAME AS RPT <input checked="" type="checkbox"/> DTIC USERS <input type="checkbox"/>		21. ABSTRACT SECURITY CLASSIFICATION Unclassified										
22a. NAME OF RESPONSIBLE INDIVIDUAL David Mann		22b. TELEPHONE NUMBER (Include Area Code) 919-549-0641	22c. OFFICE SYMBOL ARO									

UNCLASSIFIED

SECURITY CLASSIFICATION OF THIS PAGE

condition, and what enhanced heat transfer from the end gas would preclude autoconversion--though too great heat transfer from the end gas could result in flame quenching (unburned residual fuel).

Accession For	
NTIS GRA&I	<input checked="checked" type="checkbox"/>
DTIC TAB	<input type="checkbox"/>
Unannounced	<input type="checkbox"/>
Justification	
By _____	
Distribution/	
Availability Codes	
Dist	Avail and/or Special
A-1	



Unclassified

AIAA'84

AIAA-84-0208

**Modeling End-Gas Knock in a
Rapid-Compression Machine**

W.B. Bush, F.E. Fendell and S.F. Fink,
TRW Electronic and Defense Sector,
Redondo Beach, CA

AIAA 22nd Aerospace Sciences Meeting

January 9-12, 1984/Reno, Nevada

For permission to copy or republish, contact the American Institute of Aeronautics and Astronautics
1633 Broadway, New York, NY 10019

84 03 20 019

MODELING END-GAS KNOCK IN A RAPID-COMPRESSION MACHINE

W. B. Bush*, F. E. Fendell†, S. F. Fink‡
TRW Electronic and Defense Sector
Redondo Beach, CA 90278

Abstract

A rapid-compression machine is a laboratory apparatus to study aspects of the compression stroke, combustion event, and expansion stroke of an Otto cycle. As a simple model of such a machine, unsteady one-dimensional nonisobaric laminar flame propagation through a combustible premixture, enclosed in a variable volume, is examined in the asymptotic limit of Arrhenius activation temperature large relative to the conventional adiabatic flame temperature. In this limit, a thin propagating flame separates nondiffusive expanses of burned and unburned gas. The pressure through the enclosure is spatially homogeneous for smooth flame propagation. However, expansion of the hot burned gas results in compressional preheating of the remaining unburned gas, and in fact the spatially homogeneous gas may undergo autoconversion prior to arrival of the propagating flame. If such an explosion is too rapid for acoustic adjustment, large spatial differences in pressure arise and the resulting nonlinear waves produce audible knock. Here attention is concentrated on what fraction (if any) of the total charge may undergo autoconversion for a given operating condition, and what enhanced heat transfer from the end gas would preclude autoconversion--though too great heat transfer from the end gas could result in flame quenching (unburned residual fuel).

1. Introduction

During nonisobaric flame propagation through an initially homogeneous premixture of combustible gases in an (in general, variable-volume) enclosure, end-gas knock may occur. That is, the residual unburned gas is preheated prior to flame arrival by compression, owing to expansion of the already burned gas and possibly also owing to movement of the walls of the enclosure; if this preheating results in a high-enough unburned-gas temperature, virtually the entire residual gas may undergo autoignition and rapid conversion to product in a spatially homogeneous explosion. This phenomenon is known as end-gas knock; because the temporal scale of the abrupt local autoconversion may be shorter than the acoustic-wave speed, the pressure field (well approximated to be a function of time only during normal flame propagation) becomes spatially nonuniform, and the resulting nonlinear waves interact with the walls to produce loud noise. In view of the current capacity to treat the exhaust of Otto-cycle engines, the potential damage to engine components from end-gas knock is a major obstacle to operation at high thermal efficiency, i.e., at high compression ratio^{1,2}.

*Consultant, Engineering Sciences Laboratory.
†Staff Engineer, Engineering Sciences Laboratory.
‡Associate Fellow AIAA.
‡Member of the Technical Staff, Hardness and Survivability Laboratory.

Here further insight into end-gas knock is sought from a mechanical-engineering point of view, as distinct from a chemical-kinetic point of view. That is, a Shvab-Zeldovich-type* formulation of the one-dimensional unsteady laminar interplay of species and heat diffusion, exothermic chemical reaction, compressional heating, and heat loss is solved for an impervious noncatalytic variable-volume enclosure. Such a model may suffice for a so-called rapid-compression machine for cases in which ignition is arranged such that a planar flame propagates parallel to one moveable (piston-like) end wall. Often, such a machine serves as a conveniently instrumented laboratory apparatus for detailed examination of compression and reaction (and perhaps subsequent expansion as well). In contrast, in an Otto-cycle engine multiple repetitions of the entire cycle (including induction and exhaust) are entailed, the flame propagation is highly unsteady ("turbulent"), the flame is often predominantly perpendicular to the piston crown, and the range of parametric variation may in practice be constrained relatively narrowly by cost and available equipment^{3,4}.

Accordingly, the following questions are addressed: (1) under what conditions is the onset of knock to be expected in a rapid-compression machine; (2) what fraction of the initial premixture undergoes autoconversion; and (3) what heat transfer from the end gas would suffice for smooth flame propagation across the entire combustible mixture.

2. Formulation

For a low-Mach-number flow in which fuel F and oxygen O pass exothermically to product P (in the presence of nitrogen N) via

$$\nu_F F + \nu_O O + \nu_N N \rightarrow \nu_P P + \nu_N N, \quad (2.1)$$

where ν_i is the stoichiometric coefficient of species i , the dimensional conservation equations for mass, species, and energy, and state equation are taken, in the domain $0 < x^* < L^*(t^*)$, $t^* > 0$, to be^{5,6}

$$\frac{\partial \rho^*}{\partial t^*} + \frac{\partial(\rho^* u^*)}{\partial x^*} = 0; \quad \frac{\partial \psi^*}{\partial x^*} = \rho^*, \quad \frac{\partial \psi^*}{\partial t^*} = -\rho^* u^*; \quad (2.2)$$

$$\rho^* \left(\frac{\partial Y_i}{\partial t^*} + u^* \frac{\partial Y_i}{\partial x^*} \right) - \frac{\partial}{\partial x^*} \left((\rho^* D^*) \frac{\partial Y_i}{\partial x^*} \right) = -w^*,$$

$$i = F, O; Y_i = \frac{m^* \tilde{Y}_i}{m_i^* v_i^*}; \quad (2.3)$$

*In particular, a direct one-step irreversible bimolecular second-order Arrhenius-type global reaction is adopted, and no attempt is made to examine detailed chemical-kinetic rates and mechanisms.

$$\rho^* \left(\frac{\partial T^*}{\partial t^*} + u^* \frac{\partial T^*}{\partial x^*} \right) - \frac{\partial}{\partial x^*} \left((\lambda^*/c_p^*) \frac{\partial T^*}{\partial x^*} \right) =$$

$$\left(\frac{Q^*}{c_p^*} \right) w^* + \frac{1}{c_p^*} \frac{dp^*}{dt^*}; \quad (2.4)$$

$$p^* = \rho^* R^* T^*. \quad (2.5)$$

Here, t^* and x^* are the time and Cartesian spatial coordinates, respectively; u^* is the gas speed and ψ^* is the streamfunction; ρ^* and T^* are the density and the temperature; R^* is the gas constant for the mixture, taken to be composed of species of comparable molecular weight; p^* is the pressure, taken to be a function of time only from consideration of the equation of conservation of momentum; Y and m_i^* are the mass fraction and molecular weight, respectively, of species i ; $m^* = v_F m_F^* + v_O m_O^* + v_N m_N^*$; D^* and λ^* are the mass-transfer and thermal-conductivity coefficients, respectively, and c_p^* is the (constant universal) heat capacity at constant pressure; Q^* is the heat of combustion per mass of premixture; and w^* is the reaction rate. The Lewis-Semenov number is taken as a constant of order unity, i.e.,

$$Le = \frac{(\lambda^*/c_p^*)}{(\rho^* D^*)} = \text{const.} \sim O(1). \quad (2.6)$$

It is also taken that

$$\rho^* D^* \sim p^{*n} = \text{fnc}(t^*). \quad (2.7)$$

Further, consistent with the nature of the formulation,

$$w^* = B^* T_a^{*\alpha} \rho^{*v_F+v_O} Y_F^{v_F} Y_O^{v_O} \exp\left\{-T_a^*/(T^*-T_{uo}^*)\right\}, \quad (2.8)$$

where B^* is the (constant) frequency factor; T_a^* is the (constant) Arrhenius activation temperature; T_{uo}^* is the uniform initial premixture temperature, introduced to modify the Arrhenius factor so as to preclude the "cold-boundary difficulty"; and α characterizes the preexponential thermal dependence of the reaction rate. Here, $\alpha = \{(v_F+v_O)-1\}$ is adopted.

It is convenient to adopt the von Mises transformation $(x^*, t^*) \rightarrow (\psi^*, t^*)$, where the streamfunction ψ^* is defined in (2.2). Under this transformation, the species and energy conservation equations, (2.3) and (2.4), become

$$\frac{\partial Y_i}{\partial t^*} - (\rho^{*2} D^*) \frac{\partial Y_i}{\partial \psi^{*2}} = -B^* (p^*/R^*)^\alpha Y_F^{v_F} Y_O^{v_O} \times \exp\left\{-T_a^*/(T^*-T_{uo}^*)\right\}, i=F, O, \quad (2.9)$$

$$\frac{\partial T^*}{\partial t^*} - Le(\rho^{*2} D^*) \frac{\partial^2 T^*}{\partial \psi^{*2}} = \left(\frac{Q^*}{c_p^*} \right) B^* (p^*/R^*)^\alpha Y_F^{v_F} Y_O^{v_O} \times \exp\left\{-T_a^*/(T^*-T_{uo}^*)\right\} + \frac{T^*}{(c_p^*/R^*)} \frac{1}{p^*} \frac{dp^*}{dt^*}; \quad (2.10)$$

The mass conservation and mapping equations are

$$\frac{\partial u^*}{\partial \psi^*} = \frac{\partial}{\partial t^*} \left(\frac{1}{\rho^*} \right), \quad \frac{\partial x^*}{\partial \psi^*} = \frac{1}{\rho^*}. \quad (2.11)$$

For nondimensionalization,

$$t = \frac{t^*}{(L_o^*/u_{uo}^*)}, \quad \psi = \frac{\psi^*}{\rho_{uo}^* L_o^*}; \quad (2.12)$$

$$Y(\psi, t) = \frac{Y_F(\psi^*, t^*)}{Y_{Fu}} = \frac{(1-\phi)}{\phi} \left(\frac{Y_O(\psi^*, t^*)}{Y_{Ob}} - 1 \right),$$

$$T(\psi, t) = \frac{T^*(\psi^*, t^*) - T_{uo}^*}{T_{bo}^* - T_{uo}^*}; \quad (2.13)$$

$$p(t) = \frac{p^*(t^*)}{p_o^*}; \quad (2.14)$$

$$\rho(t) = \frac{\rho^*(\psi^*, t^*)}{\rho_{uo}^*}, \quad u(\psi, t) = \frac{u^*(\psi^*, t^*)}{u_{uo}^*},$$

$$x(\psi, t) = \frac{x^*(\psi^*, t^*)}{L_o^*}. \quad (2.15)$$

Here, the subscript u denotes unburned-premixture conditions, the subscript b denotes burned-state conditions at the flame, and the subscript o denotes initial conditions. Specifically, u_{uo}^* is the initial adiabatic flame speed, and T_{bo}^* is the initial adiabatic flame temperature. Also $\phi = (Y_{Fu}/Y_{Ou})$ is the equivalence ratio, with $\phi < 1$ for cases of interest, so $Y_{Fb} = 0$. Hence, with $\phi = \{\phi/(1-\phi)\}$ of order unity, $Y_{Ob} = (Y_{Ou} - Y_{Fu})/\phi$, and $T_{bo}^* = \{T_{uo}^* + (Q^*/c_p^*) Y_{Fu}\}$ (including $T_{bo}^* = T_{uo}^* + (Q^*/c_p^*) Y_{Fu}$). Note also that $p_o^* = \rho_{uo}^* R^* T_{uo}^*$.

Thus, the nondimensional species and energy equations are, for $\alpha, n = 1$, and $v_F, v_O = 1$,

$$\frac{\partial Y}{\partial t} - \epsilon p \frac{\partial^2 Y}{\partial \psi^2} = -\frac{1}{\epsilon} \Lambda_o p Y(1+\phi Y) \exp\{-\beta(1-T)/T\}, \quad (2.16)$$

$$\frac{\partial T}{\partial t} - \epsilon Le p \frac{\partial^2 T}{\partial \psi^2} = \frac{1}{\epsilon} \Lambda_o p Y(1+\phi Y) \exp\{-\beta(1-T)/T\} + \frac{(Y-1)}{Y} \frac{(1+KT)}{kp} \frac{dp}{dt},$$

where

$$\epsilon = (D_{uo}^*/u_{uo}^*)/L_o^* \ll 1, \quad (2.18)$$

$$\beta = T_a^*/(T_{bo}^* - T_{uo}^*) \gg 1, \quad K = (T_{bo}^* - T_{uo}^*)/T_{uo}^* = O(1),$$

$$\Lambda_o = (B^* D_{uo}^*/u_{uo}^{*2}) (p_o^*/R^*)^\alpha \phi^{-v_O} Y_{Fu}^\alpha \exp(-\beta) \gg 1, \quad (2.19)$$

$$\gamma = c_p^*/c_v^* = c_p^*/(c_p^* - R^*) > 1. \quad (2.20)$$

The nondimensional state, continuity, and mapping equations are

$$\rho = \frac{p}{1+KT}, \quad \frac{\partial u}{\partial \psi} = \frac{\partial}{\partial t} \left(\frac{1}{\rho} \right) = \frac{\partial}{\partial t} \left(\frac{(1+KT)}{p} \right),$$

$$\frac{\partial x}{\partial \psi} = \frac{1}{\rho} = \frac{(1+KT)}{p}. \quad (2.21a, b, c)$$

From steady (isobaric) fuel-lean laminar flame propagation, for $\beta \gg 1$, it is known that, for $v_F = 1$,

$$\Lambda_o = \frac{\beta^2}{2Le^2} \left[1 + O(\beta^{-1}) \right] \text{ for } v_F = 1, \quad (2.22)$$

where the higher-order terms are known but are not utilized here.

In this formulation, the fixed wall is located at $x = 0$; the moving wall is located at $x = L(t)$, with $L(0) \equiv 1$. Under the von Mises transformation, with the fixed wall located at $\psi = 0$, the moving wall is

located at $\psi = \psi(t)$, with $\psi(0) \equiv \psi_0 = \text{const.} > 0$, i.e.,

$$\psi = \int_0^x \rho dx_1 = p \int_0^x \frac{dx_1}{(1+KT)}; \quad (2.23a)$$

$$\psi = \int_0^L \rho dx_1 = p \int_0^L \frac{dx_1}{(1+KT)}. \quad (2.23b)$$

In general, the initial conditions for this flow geometry are

$$Y \rightarrow 1, T \rightarrow 0 \text{ (} p \rightarrow 1 \text{) as } t \rightarrow 0 \text{ for } \psi > \psi_{f0} \rightarrow 0, \quad (2.24a)$$

$$Y \rightarrow 0, T \rightarrow 1 \text{ (} p \rightarrow 1 \text{) as } t \rightarrow 0 \text{ as } \psi \rightarrow (\psi_{f0})^-, \quad (2.24b)$$

Note that, subject to (2.24), it follows from (2.23) that $\psi_0 = 1$. In general, if both walls are impermeable noncatalytic adiabatic ones, the boundary conditions are

$$\frac{\partial Y}{\partial \psi}, \frac{\partial T}{\partial \psi} \rightarrow 0, x, u \rightarrow 0 \text{ as } \psi \rightarrow 0 \text{ (} t > 0 \text{),} \quad (2.25a)$$

$$\frac{\partial Y}{\partial \psi}, \frac{\partial T}{\partial \psi} \rightarrow 0, x \rightarrow L(t), u \rightarrow L'(t) \text{ as } \psi \rightarrow 1 \text{ (} t > 0 \text{).} \quad (2.25b)^{\#}$$

The jump conditions at the flames are

$$\begin{aligned} \llbracket Y \rrbracket &= (Y_b - Y_u) = -1, \llbracket T \rrbracket = (T_b - T_u) = 1 \\ &\text{at } \psi = \psi_f(t). \end{aligned} \quad (2.26)$$

3. External Hydrodynamics of Flame Propagation

Exterior to the thin-flame structure, there is an unburned region, defined by $\psi_f(t) < \psi < 1$, and a burned region, defined by $\psi_f(t) > \psi > 0$. In both these unburned and burned regions, the diffusion and reaction-rate contributions are taken to be negligible, so that the species and energy equations, (2.16) and (2.17), reduce to

$$\frac{\partial Y}{\partial t} = 0, \frac{\partial T}{\partial t} - \frac{(\gamma-1)}{\gamma} \frac{(1+KT)}{Kp} \frac{dp}{dt} = 0. \quad (3.1,2)$$

Here, the unburned region, $\psi_f(t) < \psi < 1$, is considered to consist of a bulk-gas region, $\psi_f(t) < \psi < \psi_i$, and an end-gas region, $\psi_i < \psi < 1$, where ψ_i (given) denotes the interface, or contact surface, between the bulk gas and the end gas. This division of the unburned region holds for $0 < t < t_i$. When $t = t_i$, all the unburned bulk gas has been burned, i.e., $\psi_f(t_i) = \psi_i$.

[#]On physical grounds, since pressure is spatially invariant, results depend on wall separation as a function of time; as long as the temporal history of wall separation is the same, results are invariant to which (or both) end wall moves. Also, from (2.19) and (2.22), altering some parameters not only alters dimensionless groups, but also alters the derived quantity u_{00}^* , so that the temporal scale and the streamfunction scale used for nondimensionalization are altered. Thus, for example, altering the value of the activation temperature T_a^* changes the value of β and u_{00}^* , so not only may the value of T at any value of ψ and t (in general) be altered, but the associated dimensional quantities ψ^* and t^* are altered. Finally, in a straightforward generalization of (2.24), sparking need not occur necessarily at time $t = 0$; e.g., compressional heating owing to wall motion may occur for a finite time interval before sparking initiates flame propagation.

For $t > t_i$, the unburned region consists of just the end-gas region. To distinguish among these regions, the following notation is introduced:

unburned bulk gas

$$Y(\psi, t) = Y_u(\psi, t), T(\psi, t) = T_u(\psi, t), \quad Y = \kappa \text{ for } \psi_f(t) < \psi < \psi_i; \quad (3.3a)$$

unburned end gas

$$Y(\psi, t) = X_u(\psi, t), T(\psi, t) = (\mathcal{H})_u(\psi, t), \quad Y = \mu \text{ for } \psi_i < \psi < 1; \quad (3.3b)$$

burned bulk gas

$$Y(\psi, t) = Y_b(\psi, t), T(\psi, t) = T_b(\psi, t), \quad Y = \sigma \text{ for } \psi_i > \psi_f(t) > \psi > 0; \quad (3.3c)$$

burned end gas

$$Y(\psi, t) = X_b(\psi, t), T(\psi, t) = (\mathcal{H})_b(\psi, t), \quad Y = T \text{ for } \psi_f(t) > \psi > \psi_i. \quad (3.3d)$$

For the unburned bulk gas, (3.1) and (3.2) become

$$\frac{\partial Y_u}{\partial t} = 0, \frac{\partial T_u}{\partial t} - \frac{(\kappa-1)}{\kappa} \frac{(1+K T_u)}{Kp} \frac{dp}{dt} = 0. \quad (3.4a,b)$$

The solutions of (3.4), subject to the initial conditions for this region,

$$p(0) = 1, Y_u(\psi, 0) = 1, T_u(\psi, 0) = 0, \text{ and } \psi_f(0) < \psi < \psi_i, \quad (3.5)$$

with $\psi_f(0) = \psi_{f0} \rightarrow 0$, ψ_i const. (to be specified), are

$$Y_u(\psi, t) = 1, T_u(\psi, t) = T_u(t) = \frac{1}{K} \left[\{p(t)\}^{(\kappa-1)/\kappa} - 1 \right]. \quad (3.6a,b)$$

In a similar manner, for the unburned end gas, the solutions of

$$\frac{\partial X_u}{\partial t} = 0, \frac{\partial (\mathcal{H})_u}{\partial t} - \frac{(\mu-1)}{\mu} \frac{(1+K (\mathcal{H})_u)}{Kp} \frac{dp}{dt} = 0, \quad (3.7a,b)$$

subject to the initial conditions

$$p(0) = 1, X_u(\psi, 0) = 1, (\mathcal{H})_u(\psi, 0) = 0, \text{ and } \psi_i < \psi < 1, \quad (3.8)$$

are

$$X_u(\psi, t) = 1, (\mathcal{H})_u(\psi, t) = (\mathcal{H})_u(t) = \frac{1}{K} \left[\{p(t)\}^{(\mu-1)/\mu} - 1 \right]. \quad (3.9a,b)$$

For the burned-bulk-gas region, (3.1) and (3.2) become

$$\frac{\partial Y_b}{\partial t} = 0, \frac{\partial T_b}{\partial t} - \frac{(\sigma-1)}{\sigma} \frac{(1+K T_b)}{Kp} \frac{dp}{dt} = 0. \quad (3.10a,b)$$

The solutions are of the forms

$$Y_b(\psi, t) = H_b(\psi), T_b(\psi, t) = \frac{1}{K} \left[F_b(\psi) \{p(t)\}^{(\sigma-1)/\sigma} - 1 \right].$$

At the flame,

$$Y_b(\psi_f(t), t) = H_b(\psi_f(t)) : Y_{bf}(t) = H_{bf}(t), \quad (3.11a,b)$$

$$T_b(\psi_f(t), t) = \frac{1}{K} \left[F_b(\psi_f(t)) \{p(t)\}^{(\sigma-1)/\sigma} - 1 \right] :$$

$$T_{bf}(t) = \frac{1}{K} \left[F_{bf}(t) \{p(t)\}^{(\sigma-1)/\sigma} - 1 \right]. \quad (3.12b)$$

For $t < t_i$ and/or $\psi_f(t) < \psi_i$, the jump conditions at the flame (between the unburned bulk gas and the burned bulk gas) yield

$$Y_{bf}(t) = 0 \Rightarrow Y_b(\psi, t) = 0, \quad (3.13a)$$

$$T_{bf}(t) = \{1 + T_u(t)\} \Rightarrow F_{bf}(t) = \frac{\{p(t)\}^{(\kappa-1)/\kappa + K}}{\{p(t)\}^{(\sigma-1)/\sigma}}. \quad (3.13b)$$

Similarly for $t > t_i$, and/or $\psi_f(t) > \psi_i$,

$$x_b(\psi, t) = 0, \quad \textcircled{H}_b(\psi, t) = \frac{1}{K} \left[G_b(\psi) \{p(t)\}^{(T-1)/T} - 1 \right];$$

$$\textcircled{H}_{bf}(t) = \frac{1}{K} \left[G_{bf}(t) \{p(t)\}^{(T-1)/T} - 1 \right]. \quad (3.14a, b, c)$$

Also,

$$\textcircled{H}_{bf}(t) = \{1 + \textcircled{H}_u(t)\} \Rightarrow G_{bf}(t) = \frac{\{p(t)\}^{(\mu-1)/\mu + K}}{\{p(t)\}^{(T-1)/T}}.$$

3.1 $\psi_f(t) < \psi_i$ (Flame in the Bulk Gas)

For $t < t_i$ and/or $\psi_f(t) < \psi_i$, integration of the mapping equation, (2.21a), over the domain $0 \leq \psi \leq 1$ yields

$$\int_0^{L(t)} dx = \int_0^{\psi_f(t)} \frac{\{1 + K T_b(\psi, t)\}}{p(t)} d\psi +$$

$$\int_{\psi_f(t)}^{\psi_i} \frac{\{1 + K T_u(\psi, t)\}}{p(t)} d\psi + \int_{\psi_i}^1 \frac{\{1 + K \textcircled{H}_u(\psi, t)\}}{p(t)} d\psi;$$

$$L(t) = \frac{1}{\{p(t)\}^{1/\sigma}} \int_0^{\psi_f(t)} F_b(t) d\psi +$$

$$\frac{\{\psi_i - \psi_f(t)\}}{\{p(t)\}^{1/\kappa}} + \frac{(1 - \psi_i)}{\{p(t)\}^{1/\mu}}. \quad (3.15)$$

Upon multiplication by $\{p(t)\}^{1/\sigma}$, the time derivative of (3.15), with rearrangement, produces

$$\frac{1}{\sigma} \frac{p'(t)}{p(t)} \left[1 - \frac{(\kappa - \sigma)}{\kappa} \frac{\{\psi_i - \psi_f(t)\}}{L(t) \{p(t)\}^{1/\kappa}} - \right.$$

$$\left. \frac{(\mu - \sigma)}{\mu} \frac{(1 - \psi_i)}{L(t) \{p(t)\}^{1/\mu}} \right] + \frac{L'(t)}{L(t)} - \frac{K \psi_f'(t)}{L(t) p(t)} = 0. \quad (3.16)$$

Integration of the mapping equation over the unburned domain $\psi < \psi_i < 1$, with $\psi \geq \psi_f(t)$, yields

$$\int_{x_u(\psi, t)}^{L(t)} dx = \int_{\psi}^{\psi_i} \frac{\{1 + K T_u(\psi_1, t)\}}{p(t)} d\psi_1 +$$

$$\int_{\psi_i}^1 \frac{\{1 + K \textcircled{H}_u(\psi_1, t)\}}{p(t)} d\psi_1;$$

$$x_u(\psi, t) = L(t) - \frac{(\psi_i - \psi)}{\{p(t)\}^{1/\kappa}} - \frac{(1 - \psi_i)}{\{p(t)\}^{1/\mu}}. \quad (3.17)$$

Note that

$$x_u(\psi_f(t), t) = x_f(t) = L(t) - \frac{\{\psi_i - \psi_f(t)\}}{\{p(t)\}^{1/\kappa}} - \frac{(1 - \psi_i)}{\{p(t)\}^{1/\mu}}. \quad (3.18)$$

In turn,

$$\frac{\partial x_u}{\partial t}(\psi, t) = u_u(\psi, t) = L'(t) + \frac{p'(t)}{p(t)} \left[\frac{1}{\kappa} \frac{(\psi_i - \psi)}{\{p(t)\}^{1/\kappa}} + \right.$$

$$\left. \frac{1}{\mu} \frac{(1 - \psi_i)}{\{p(t)\}^{1/\mu}} \right], \quad (3.19)$$

$$\frac{dx_f}{dt}(t) = x_f'(t) = L'(t) + \frac{p'(t)}{p(t)} \left[\frac{1}{\kappa} \frac{\psi_i - \psi_f(t)}{\{p(t)\}^{1/\kappa}} + \right.$$

$$\left. \frac{1}{\mu} \frac{(1 - \psi_i)}{\{p(t)\}^{1/\mu}} \right] + \frac{\psi_f'(t)}{\{p(t)\}^{1/\kappa}}. \quad (3.20)$$

Thus, the flame speed, the difference between the speed of the flame front and that of the unburned gas at the flame front, is

$$S = S(t) = \left[x_f'(t) - \lim_{\psi \rightarrow \psi_f(t)} \{u_u(\psi, t)\} \right] = \frac{\psi_f'(t)}{\{p(t)\}^{1/\kappa}}. \quad (3.21)$$

In Appendix A, it is determined that, for $\alpha, n = 1$ and $v_0, v_f = 1$, the flame speed is

$$S(t) = \{1 + K T_u(t)\} \{1 + T_u(t)\}^2 \exp \left[\beta T_u(t) / 2 \{1 + T_u(t)\} \right]. \quad (3.22)$$

It may be shown that $\{\partial x_u(\psi, t) / \partial t\} = u_u(\psi, t)$ is continuous at $\psi = \psi_i$, i.e., is continuous across the contact surface between the unburned-bulk-gas region and the unburned-end-gas region.

Thus, with the motion of the moving wall, i.e., $L(t)$ and $L'(t)$ and the interface location ψ_i specified, the pertinent initial-value problem becomes (3.6b), (3.9b), (3.16), (3.21), and (3.22), subject to

$$p(0) = 1, \quad T_u(0) = 0, \quad (3.23)^\dagger$$

[†] From (3.16) and (3.23) for $L' = 0$, $\kappa = \sigma$, $\psi_i = 1$, one recovers the following classical results, if $p = p_1$ when $\psi_f = 1$:

$$p(t) - 1 = \sigma K \psi_f(t) \Rightarrow p_1 - 1 = \sigma K \Rightarrow \frac{p(t) - 1}{p_1 - 1} = \psi_f(t).$$

This implies that the peak value of T_u is

$$(T_u)_{\max} = \frac{1}{K} \left[\{1 + \sigma K\}^{(\kappa-1)/\kappa} - 1 \right].$$

This problem terminates when $t = t_i$, such that

$$p(t_i) = p_i, T_u(t_i) = T_{ui}, \quad \textcircled{H}_u(t_i) = \textcircled{H}_{ui}, \quad \psi_f(t_i) = \psi_i, \quad (3.24)$$

where $p_i, T_{ui}, \textcircled{H}_{ui}$ are found in the course of solution. Here, the motion of the moving wall is approximated as

$$L(t) = \left[1 - \left\{ \frac{(CR) - 1}{2(CR)} \right\} (1 - \cos \omega t) \right],$$

$$L'(t) = -\left\{ \frac{(CR) - 1}{2(CR)} \right\} (\omega \sin \omega t), \quad (3.25a, b)$$

where $(CR)(>1)$ is the compression ratio (L_{\max}/L_{\min}) = $(1/L_{\min})$, and $\omega (= 2\pi\Omega = 2\pi\{\Omega^*/(u_{00}^*/L_0^*)\})$, with Ω^* the number of revolutions per unit time) is the (nondimensional) frequency.

3.2 $\psi_f(t) > \psi_i$ (Flame in the End Gas)

For $t > t_i$ and/or $\psi_f(t) > \psi_i$, integration of the mapping equation, (2.21a), over the domain $0 \leq \psi \leq 1$ yields

$$L(t) = \frac{1}{\{p(t)\}^{1/\sigma}} \int_0^{\psi_i} F_b(\psi) d\psi + \frac{1}{\{p(t)\}^{1/T}} \int_{\psi_i}^{\psi_f(t)} G_b(\psi) d\psi +$$

$$\frac{\{1 - \psi_f(t)\}}{\{p(t)\}^{1/\mu}}. \quad (3.26)$$

Thus, for this case,

$$\frac{1}{\sigma} \frac{p'(t)}{p(t)} \left[1 - \frac{(\mu - \sigma)}{\mu} \frac{\{1 - \psi_f(t)\}}{L(t)\{p(t)\}^{1/\mu}} - \right.$$

$$\left. \frac{\int_{\psi_i}^{\psi_f(t)} G_b(\psi) d\psi}{L(t)\{p(t)\}^{1/T}} \right] + \frac{L'(t)}{L(t)} - \frac{K\psi_f'(t)}{L(t)p(t)} = 0, \quad (3.27)$$

where it is approximated that

$$\int_{\psi_i}^{\psi_f(t)} G_b(\psi) d\psi = \frac{\{\psi_f(t) - \psi_i\}}{2} \{G_b(\psi_f(t)) + G_b(\psi_i)\}, \quad (3.28a)$$

$$G_b(\psi_f(t)) = \frac{\{p(t)\}^{(\mu-1)/\mu} + K}{\{p(t)\}^{(T-1)/T}}, \quad G_b(\psi_i) = \frac{p_i^{(\mu-1)/\mu} + K}{p_i^{(T-1)/T}}. \quad (3.28b)$$

Integration of the mapping equation over the (end-gas) unburned domain $\psi < 1$, with $\psi \geq \psi_f(t)$, yields

$$x_u(\psi, t) = L(t) - \frac{(1 - \psi)}{\{p(t)\}^{1/\mu}}, \quad x_u(\psi_f(t), t) = x_f(t) =$$

$$L(t) - \frac{\{1 - \psi_f(t)\}}{\{p(t)\}^{1/\mu}}. \quad (3.29a, b)$$

In turn,

$$\frac{\partial x}{\partial t}(\psi, t) = u_u(\psi, t) = L'(t) + \frac{p'(t)}{p(t)} \left[\frac{1}{\mu} \frac{(1 - \psi)}{\{p(t)\}^{1/\mu}} \right],$$

$$\frac{dx_f}{dt}(t) = x_f'(t) = L'(t) + \frac{p'(t)}{p(t)} \left[\frac{1}{\mu} \frac{\{1 - \psi_f(t)\}}{\{p(t)\}^{1/\mu}} \right] +$$

$$\frac{\psi_f'(t)}{\{p(t)\}^{1/\mu}}. \quad (3.30)$$

Thus, the flame speed is

$$S = S(t) = \left[x_f'(t) - \lim_{\psi \rightarrow \psi_f(t)} \{u_u(\psi, t)\} \right] = \frac{\psi_f'(t)}{\{p(t)\}^{1/\mu}}, \quad (3.31)$$

where, for $\alpha, n = 1$ and $v_0, v_f = 1$,

$$S(t) = \left\{ 1 + K \textcircled{H}_u(t) \right\} \left\{ 1 + \textcircled{H}_u(t) \right\}^2 \times$$

$$\exp \left[\beta \textcircled{H}_u(t) / 2 \left\{ 1 + \textcircled{H}_u(t) \right\} \right]. \quad (3.32)$$

Thus, for this domain, the pertinent initial-value problem is given by (3.9b), (3.27), (3.28) (3.31), and (3.32), where

$$p(t_i) = p_i, \textcircled{H}_u(t_i) = \textcircled{H}_{ui}, \quad \psi_f(t_i) = \psi_i. \quad (3.33)$$

The problem nominally terminates when $t = t_1$, such that

$$p(t_1) = p_1, \textcircled{H}_u(t_1) = \textcircled{H}_{u1}, \quad \psi_f(t_1) = 1. \quad (3.34)$$

The above generalization of earlier, variable-volume-enclosure work⁷ entails a flame speed which is derived from the adopted reaction rate (cf. Senachin and Babkin⁸) and which reduces to the laminar isobaric value as $t \rightarrow 0$ (cf. Shvashinsky⁹).

4. Discussion

First, in Appendix B it is shown that for circumstances of interest, heat transfer (to slippery noncatalytic side walls) may be simulated conveniently by assignment of values to the polytropic constants κ, μ, σ , and T ; i.e., the polytropic constants effectively are equivalent to introduction of heat-transfer coefficients. The smaller the value assigned to a polytropic constant, the greater the heat transfer in the associated domain. While adequate experimental identification of polytropic constants (or heat-transfer coefficients) seems yet to be reported in the literature, the consequences of assigning relative values permits comparison of heat-transfer requirements for varying parametric conditions.

Second, in singular-perturbation terms, end-gas knock is the physical manifestation of the possible nonuniform validity in time of the asymptotic approximation (based on $\beta \gg 1$) that the reaction-rate contribution is negligible in the unburned gas; however, the asymptotic approximation (based on $\epsilon \ll 1$) that the diffusion contribution is negligible remains uniformly valid. Thus, if one retains chemical reaction terms in (2.16) that were discarded in writing (3.1,2) because the terms were taken as exponentially small, then one has

$$\frac{\partial Y}{\partial t} = -\frac{1}{\epsilon} \Lambda_0 p Y (1 + \phi Y) \exp\{-\beta(1-T)/T\}, \quad (4.1)$$

$$\frac{\partial T}{\partial t} = \frac{1}{\epsilon} \Lambda_0 p Y (1 + \phi Y) \exp\{-\beta(1-T)/T\} + \frac{(\gamma-1)}{\gamma} \frac{(1+KT)}{Kp} \frac{dp}{dt}, \quad (4.2)$$

where $(Y(\psi, t), T(\psi, t), \gamma) \rightarrow (Y_u(t), T_u(t), \kappa)$ in the unburned-bulk-gas region and $(Y(\psi, t), T(\psi, t), \gamma) \rightarrow (X_u(t), (H)_u(t), u)$ in the unburned-end-gas region. It is recalled that adjustment of the polytropic constant γ simulates the effect of heat loss. The above problem, subject to the initial conditions $Y(0) = 1, T(0) = 0$, is a variant of the classical spatially homogeneous, nonstationary ignition problem, in which the criterion for an explosion self-sustained against heat loss is sought. Here compressional heating, as reflected in the pressure $p(t)$ raises the temperature of the premixture; clearly, as T rises in time, the reaction-rate term may become comparable to the other terms in the energy equation. If one substitutes the pressure, $p(t)$, from solution of the problem posed in Section 3, then one can obtain an indication from (4.1) and (4.2) whether significant autoconversion occurs in the end gas prior to completion of flame propagation. If modest autoconversion causes pressure rise in time during flame transit beyond that accounted for in the theory of Section 3, that development is not easily generalized to include it. Of more concern is very significant autoconversion of unburned gas on a time scale comparable to, or less than, the time scale for completion of flame propagation. Especially if the time scale is less than that for completion of flame propagation (and less than that for acoustic adjustment), there occurs effectively a constant-volume explosion of the unburned gas. Such a relatively instantaneous reaction of unburned gas results in a pressure in the end-gas region higher than the pressure in the rest of the gas. The consequence is nonlinear pressure waves, and an audible sound from sympathetic vibration of engine components. However, there is no incentive to pursue solution into this spatially-nonuniform-pressure domain because the above formulation is inadequate.

Standard asymptotic solution for $\beta \gg 1$ of (4.1) and (4.2), or even of (4.2) with reactant consumption ignored (i.e., $Y \equiv 1$), suffices to establish that, for plausible parameter assignments for hydrocarbon-air premixtures of automotive interest, autoconversion becomes effectively instantaneous relative to flame-propagation speed over (say) a half centimeter for unburned gas temperature on the order of 1025 K; practical experimental data for nonisobaric combustion also give this value.¹ Mathematical treatment beyond that in Appendix C seems of limited engineering utility.

Thus, the following computational procedure is evolved to answer the questions posed in the last paragraph of Section 1. First, with κ, σ taken as given and ψ_i set equal to unity (so there is no end gas), the first initial-value problem posed in Section 3 is carried out for the parametric assignments of interest. If it holds uniformly in time that the temperature of the unburned gas $T_u^* < 1025$ K (for specificity), then knock is taken not to occur. If, however, T_u^* reaches 1025 K for $\psi_f(t) < 1$, then that value of ψ_f is taken as ψ_i ; i.e., ψ_i is the fraction of the charge identified as bulk gas and $(1-\psi_i)$ as end gas. Then, with T taken as given, by trial and error, the largest value of μ is sought for which $(H)_u \rightarrow 1025$ K as $\psi_f \rightarrow 1$. That is, the minimal

amount of heat transfer from the end gas is sought such that significant end-gas autoconversion barely is precluded. In this manner, the fraction (if any) of the charge that would undergo rapid autoconversion is identified, and the relative heat-transfer provision to preclude such autoconversion is determined.

In the present formulation, with adiabatic end walls, heat transfer is effected through (noncatalytic slippery) side walls. Incorporation of finite heat transfer through end walls would necessitate introduction of thermally diffusive layers in the vicinity of $\psi = 0, 1$; while such boundary layers would thicken in time, they would remain thin relative to the flow-domain length, for the time span and the parametric assignments of interest ($\epsilon \ll 1$). Such end-wall quench layers have been examined in other contexts; their introduction in the present context would seem to incur nonessential complication, such as end gas in a nonuniform thermodynamic state. The only precaution (already noted) is that very excessive heat transfer from the end-gas could so retard flame propagation that expansional cooling (from piston motion) would leave residual unburned premixture on time scales of practical interest.

5. Computational Examples

A limited number of examples now are presented of the procedure discussed in the penultimate paragraph of Section 4. For brevity of reference, the following assignment of (mainly) dimensional parameters is termed nominal:

$$\begin{aligned} T_{uo}^* &= 300 \text{ K}, T_{bo}^* = 1800 \text{ K}, T_a^* = 15,000 \text{ K}, \phi = 0.8, \\ D_{uo}^* &= 0.1 \text{ cm}^2/\text{s}, u_{uo}^* = 40 \text{ cm/s}, L_o^* = 10 \text{ cm}, Le = 1, \\ \Omega^* &= 20 \text{ rev/s}. \end{aligned} \quad (5.1)$$

It is consistent with these assignments to adopt the following "nominal" values for dimensionless parameters (the parameter ϵ does not enter the calculations--its value is given only for completeness):

$$\begin{aligned} \beta &= 10, \Lambda = 50, K = 5, \phi = 4, \epsilon = 2 \times 10^{-4}, \omega \approx 31.4, \\ \mu &= 1.4, \kappa = 1.4, T = 1.4, \sigma = 1.4, CR = 6, \theta_{ig} = 135^\circ. \end{aligned} \quad (5.2)$$

The last assignment, alluded to earlier in the footnote to (2.25b), implicitly gives the time of sparking, more precisely, the time at which flame propagation commences. That is, it is defined that

$$\theta = \omega t, \quad (5.3)$$

so at the beginning of compression $t = 0$, it holds that $\theta = 0$, which corresponds to "bottom dead center" [$L = 1$, the maximum value of L , from (3.25a)]. At $\theta = \theta_{ig}$, assigned, i.e., at $t_{ig} = \theta_{ig}/\omega$, the variables $\psi_f(t)$ and $x_f(t)$, held at zero for $0 < t < t_{ig}$, take on values consistent with (3.21) and (3.18). While sparking and compression could commence simultaneously so $t_{ig} = \theta_{ig} = 0$, in general sparking occurs after a finite interval of compression, so $t_{ig} > 0$. In the nominal case, $\theta_{ig} = 135^\circ$, or flame propagation commences after about (6/7) of the length of the (compressional) stroke. All parameters are held at their nominal values through the computations unless it is explicitly stated otherwise.

Onset of knock is taken to occur at $T_u = 0.4$, or, from (5.1), at a temperature of 900 K--a value slightly lower than that cited elsewhere in this paper.

The nominal case is found (by design) to be just barely knock-free. Computation indicates that combustion is completed at $t \approx 0.088$; since the basis of nondimensionalization is $(L_0^*/u_{00}^*) = 0.25$ s, combustion lasts 22 ms, or about three-to-four times longer than in a typical Otto-cycle-type automotive engine. At the completion of burning, $T_u \approx 0.399$, $p \approx 46.6$, $\theta \approx 157^\circ$, $L = 0.197$, whereas at the start of burning $t = 0.075$, $T_u = 0.129$, $p = 5.69$, $L = 0.289$. As with all cases to be examined, combustion is completed during the compression stroke, i.e., the crank angle $\theta < 180^\circ$; of course, in an automotive context the combustion interval is likely to be (very roughly) symmetric with respect to the time of piston position at top center.

If the polytropic constant of the burned gas σ is reduced in value from 1.4 to 1.1, all other parameters being held fixed, then at the completion of burning $t = 0.089$, $T_u = 0.378$, $p = 40.945$, $\theta = 159.8^\circ$, $L = 0.192$, whereas at the start of burning the corresponding values are (of course) those given in the preceding paragraph. Since modifying the heat transfer from the burned gas is seen to have but modest effect on the temperature of the unburned gas, this parametric variation is not pursued here further.

Table 1 presents results for four parametric variations, all selected to incur knock. The heat-transfer requirement from the end gas that precludes knock is identified in the form of the maximum value of μ (denoted μ_{crit}) that still permits $(H_u) < 0.4$ at all times during the combustion event. Further results for the case $CR = 12$ are presented in Figs. 1-3, and further results for the case $K = 3$, in Fig. 4-6; the other two variations examined are $\theta_{ig} = 165^\circ$ and $\omega = 51.6$. These cases entail between 13% and 57% of the initial combustible mass being involved in autoconversion (in the absence of augmented end-gas heat transfer), and in this sense represent a spectrum of cases. On Figs. 2, 3, 5, and 6 it may be recalled that $x_i(t)$, the interface between the unburned end gas and the unburned bulk gas, is not defined for $x_f(t) > x_i(t)$, and accordingly is neither computed nor plotted. It may be noted that the larger the fraction of end gas (i.e., the smaller the value of ψ_i), the larger the heat-transfer requirement to preclude knock (i.e., the smaller the value of μ_{crit}). However, it is noteworthy that reduction of K (from its nominal value of 5) to 3, while β is held constant, implies T_u^* is altered from 300 K to 450 K; since $T_u = 0.4$ is retained as a knock criterion, $T^* = 990$ K becomes the temperature for explosive conversion of reactant to product gas.

As a cautionary note concerning other parametric variations, it may be noted, for example, that if Y_{Fu} is altered, then ϕ and T_{b0} are altered, from the discussion below (2.15); hence, β , Λ , and K are altered from (2.19) and (2.22), but also u_{00}^* (utilized in the nondimensionalization of time t^* and the piston-speed parameter Ω^*) is altered from (2.19).

6. Concluding Remarks

The present development has concentrated on enhancing heat transfer as a countermeasure to end-gas knock. Another (perhaps complementary) strategy is to seek fuel additives that inhibit end-gas autoconversion without impeding flame propagation. While trial-and-error testing yielded the knock-inhibiting fuel additives of the past (such as tetraethyl lead, now constrained from use because it

poisons exhaust-gas-treating catalysts), it remains to be seen whether retention¹¹ of detailed chemical-kinetic rates and mechanisms for fuels of practical interest can assist identification of a substitute, environmentally acceptable knock-inhibiting additive.^{##}

Appendix A. Flame-Zone Structure

As in the unbounded (isobaric) case, the structure of the flame zone for the bounded (non-isobaric, enclosed) case for $\epsilon \ll 1$, with $\beta \gg 1$, consists of two regions: a convective-diffusive region, and a diffusive-reactive region. The results presented are for $\alpha, n = 1$ and $v_F, v_0 = 1$.

For the convective-diffusive region, the appropriate transformation of variables is $(\psi, t) \rightarrow (\xi, t)$, where

$$\xi(\psi, t; \dots) = M(t)E(t; \beta) \left[\frac{\psi_f(t) - \psi}{\epsilon} \right]. \quad (A.1)$$

The domain of this region is $-\infty < \xi < 0$, $t > 0$, such that the unburned exterior region is approached as $\xi \rightarrow -\infty$. Further, the flame speed is taken to be

$$S(t; \dots) = \psi_f'(t; \dots) / \{p(t)\}^{1/\kappa} = V(t)E(t, \beta) \left[1 + O(\beta^{-1}) \right]. \quad (A.2)$$

Here,

$$E(t; \beta) = \exp \left[\beta(T_b(t) - 1) / 2T_b(t) \right] = \exp \left[\beta T_u(t) / 2\{1 + T_u(t)\} \right]; \quad (A.3)$$

$$M(t) = \{T_b(t)\}^2 = \{1 + T_u(t)\}^2, \quad (A.4a)$$

$$V(t) = \{p(t)\}^{(\kappa-1)/\kappa} \{T_b(t)\}^2 = \{1 + K T_u(t)\} \{1 + T_u(t)\}^2. \quad (A.4b)$$

Note that $\xi \rightarrow (-\psi)/\epsilon$ and $S \rightarrow 1$ as $t \rightarrow 0$, such that the unbounded case is the initial condition of the bounded case. It is through the matching of the solutions of this convective-diffusive region with those of the diffusive-reactive region that it is

^{##}The evolution of a planar flame propagating through a not-too-far-from-stoichiometric premixture enclosed in a long-enough constant-volume duct to a so-called tulip^{12,13} shape may be evidence of a "mini-knock" event.¹⁴ It is observed that such a flame ultimately propagates less rapidly in a duct at midheight (relative to near-ceiling and near-floor flame position). Although the temperature in the compressionally-heated unburned gas may not exceed about 600 K in such tests, perhaps cool-flame (and possibly other subsequent, modestly exothermic, low-temperature) reactions engender enough end-gas counterflow to the deflagration-wave speed that flame progression is retarded at duct midheight; presumably friction inhibits the counterflow near ceiling and floor, so the flame locally propagates relatively unimpeded. Incidentally, for long-enough tubes, or for tubes of small-enough cross section, spatial gradients of pressure plausibly arise such that the tulip-flame-shape effect could be observed even if the extremity of the tube near the burned (or even unburned) premixture were open to the atmosphere.¹² Since the end-gas temperatures are typically over 1000 K for knock, the significance of cool-flame (and possibly other subsequent low-temperature) reactions in rapid-compression machines under knocking conditions is unclear.

demonstrated that (A.2) is the correct asymptotic representation of the flame speed.

For this region, the dependent variables are of the forms

$$Y(\psi, t; \dots) = X(\xi, t; \dots) \left[1 + O(\beta^{-1}) \right], \quad (A.5a)$$

$$T(\psi, t; \dots) = F(\xi, t; \dots) \left[1 + O(\beta^{-1}) \right]. \quad (A.5b)$$

Thus, for these scalings, the specific time-derivative terms and the reaction-rate terms can be neglected, such that, to leading order of approximation, (2.16) and (2.17) become

$$\frac{\partial^2 X}{\partial \xi^2} - \frac{\partial X}{\partial \xi} = 0, \quad (A.6)$$

$$Le \frac{\partial^2 F}{\partial \xi^2} - \frac{\partial F}{\partial \xi} = 0. \quad (A.7)$$

The boundary conditions for these equations are

$$X \rightarrow 1, F \rightarrow T_u \text{ as } \xi \rightarrow -\infty; \quad (A.8a)$$

$$X \rightarrow 0, F \rightarrow T_b = (1 + T_u) \text{ as } \xi \rightarrow 0. \quad (A.8b)$$

The solutions of these convective-diffusive-region boundary-value problems are

$$X(\xi, t) = \left[1 - \exp(\xi) \right], \quad (A.9)$$

$$F(\xi, t) = \left[T_u(t) + \exp(\xi/Le) \right] = T_b(t) - \left[1 - \exp(\xi/Le) \right]. \quad (A.10)$$

It is seen that

$$X \rightarrow 1, F \rightarrow T_u \text{ (exponentially) as } \xi \rightarrow -\infty, \quad (A.11)$$

and that

$$X \sim -\xi(1 + \dots) \rightarrow 0^+ \quad (A.12a)$$

$$F \sim T_b + (\xi/Le)(1 + \dots) \rightarrow T_b \text{ as } \xi \rightarrow 0^-. \quad (A.12b)$$

For the diffusive-reactive region, the transformation of variables is $(\psi, t) \rightarrow (\eta, t)$, where

$$\eta(\psi, t, \dots) = E(t; \beta) \left[\{\psi_f(t) - \psi\} / \beta^{-1} \epsilon \right], \quad (A.13)$$

where $E(t; \beta)$ is given in (A.3). The domain of this region is $-\infty < \eta < \infty$, $t > 0$, such that the burned exterior region is approached as $\eta \rightarrow \infty$. The flame speed is still that given in (A.2) *et seq.* Again, note that, as $t \rightarrow 0$, $\eta \rightarrow (-\psi) / \beta^{-1} \epsilon$ and $S \rightarrow 1$.

For this region, the dependent variables are taken to be

$$Y(\psi, t; \dots) = \beta^{-1} \{T_b(t)\}^2 Z(\eta, t; \dots) \left[1 + O(\beta^{-1}) \right] = \beta^{-1} \{1 + T_u(t)\}^2 Z(\eta, t; \dots) \left[1 + O(\beta^{-1}) \right], \quad (A.14a)$$

$$\begin{aligned} T(\psi, t; \dots) &= T_b(t) - \beta^{-1} \{T_b(t)\}^2 G(\eta, t; \dots) \left[1 + O(\beta^{-1}) \right] \\ &= \{1 + T_u(t)\} - \beta^{-1} \{1 + T_u(t)\}^2 G(\eta, t; \dots) \times \\ &\quad \left[1 + O(\beta^{-1}) \right]. \end{aligned} \quad (A.14b)$$

For $\epsilon \ll 1$ and $\beta \gg 1$, under these scalings, to leading order of approximation, for this region, the convective terms can be neglected, and (2.16) and (2.17) become

$$\frac{\partial^2 Z}{\partial \eta^2} = \frac{1}{2Le^2} Z \exp(-G), \quad (A.15)$$

$$Le \frac{\partial^2 G}{\partial \eta^2} = \frac{1}{2Le^2} Z \exp(-G). \quad (A.16)$$

The boundary conditions are

$$Z, G \rightarrow 0 \text{ as } \eta \rightarrow \infty; \quad (A.17a)$$

$$Z, G \rightarrow \infty \text{ as } \eta \rightarrow -\infty. \quad (A.17b)$$

By subtraction of (A.16) from (A.15) and use of (A.17), $Z = LeG$. Then (A.15)-(A.17) reduce to

$$\frac{\partial^2 G}{\partial \eta^2} = \frac{1}{2Le^2} G \exp(-G); \quad (A.18a)$$

$$G \rightarrow 0 \text{ as } \eta \rightarrow \infty, G \rightarrow \infty \text{ as } \eta \rightarrow -\infty. \quad (A.18b)$$

The first integral of this equation is

$$\frac{\partial G}{\partial \eta} = -\frac{1}{Le} \left[1 - (1 + G) \exp(-G) \right]^{1/2}. \quad (A.19)$$

Thus, it is determined that

$$G \sim \{\exp(-\eta/2^{1/2} Le)\} \{1 + \dots\} \rightarrow 0 \text{ as } \eta \rightarrow \infty; \quad (A.20a)$$

$$G \sim -(\eta/Le) \{1 + \dots\} \text{ as } \eta \rightarrow -\infty. \quad (A.20b)$$

Upon returning to the original dependent variables, it is seen that, for the convective-diffusive-region and diffusive-reactive-region solutions

$$Y \sim \left[(-\xi) + \dots \right] + \dots \text{ as } \xi \rightarrow 0^-,$$

$$Y \sim \beta^{-1} \left[(1 + T_u)^2 \{(-\eta) + \dots\} \right] + \dots \text{ as } \eta \rightarrow -\infty. \quad (A.21a)$$

$$T \sim \left[(1 + T_u) - (-\xi/Le) + \dots \right] + \dots \text{ as } \xi \rightarrow 0^-,$$

$$T \sim (1 + T_u) - \beta^{-1} \left[(1 + T_u)^2 \{(-\eta/Le) + \dots\} \right] + \dots \text{ as } \eta \rightarrow -\infty. \quad (A.21b)$$

Since $\eta = \beta \xi / (1 + T_u)^2$, the solution for these two regions, which involved the specification of the leading-order approximation of the flame speed, match. In the text, this flame speed, expressed as

$$\begin{aligned} S(t) &= S(T_u(t); \beta, K) = \\ &= \{1 + K T_u(t)\} \{1 + T_u(t)\}^2 \exp \left[\beta T_u(t) / 2 \{1 + T_u(t)\} \right], \end{aligned} \quad (A.22)$$

is employed.

Appendix B. Polytropic Law to Simulate Heat Transfer During the Combustion Event in an Enclosure

If the use of a super asterisk to denote a dimensional quantity is dispensed with in this appendix, then, in conventional notation, from thermodynamics,

$$c_v \frac{dT}{dt} + p \frac{d(1/p)}{dt} = q, \quad (B.1)$$

where q denotes the rate of heat addition per unit mass in the enclosure. Hence, for an ideal gas,

$$\frac{d(\gamma n T)}{dt} - (\gamma - 1) \frac{d(\gamma n p)}{dt} = \frac{q}{c_v T} \quad (B.2)$$

For tractability, let $q = -\epsilon c_v T$, with the constant $\epsilon > 0$; the product ϵc_v plays the role of a heat-transfer coefficient.^v Then, if subscript 0 denotes the initial state,

$$\frac{d}{dt} \left[\gamma n \left(\frac{p}{\rho} \right) \right] = -\epsilon \Rightarrow \frac{p}{\rho} = \frac{p_0}{\rho_0} \exp(-\epsilon t). \quad (B.3)$$

During combustion, as a rough approximation, if the constant $\mu > 0$, with μ distinct from that of (3.3b),

$$\frac{p}{p_0} \approx \exp(\mu t) \Rightarrow \frac{1}{\mu} \ln \left(\frac{p}{p_0} \right) = t; \quad (B.4)$$

hence, substitution for t by means of (B.4) gives

$$\exp(-\epsilon t) = \exp \left[-\frac{\epsilon}{\mu} \ln \left(\frac{p}{p_0} \right) \right] = \left(\frac{p}{p_0} \right)^{-\epsilon/\mu}. \quad (B.5)$$

Use of (B.5) in (B.3) gives

$$\left(\frac{p}{p_0} \right)^{1+(\epsilon/\mu)} = \left(\frac{p}{p_0} \right)^{\gamma} \Rightarrow \frac{p}{p_0} = \left(\frac{p}{p_0} \right)^{1/\gamma_*}, \quad (B.6)$$

$$\frac{1}{\gamma_*} = \frac{1}{\gamma} \left(1 + \frac{\epsilon}{\mu} \right).$$

Since $(\epsilon/\mu) > 0$, $\gamma > \gamma_*$. That is, the effect of heat transfer from a flow with rising pressure may be simulated by adoption of the polytropic constant reduced from the adiabatic value. Furthermore, via (B.6), the polytropic constant may be related to the heat-transfer coefficient (and a characterization of the rate of pressure rise).

Appendix C. End-Gas-Autoconversion Criterion

In (2.16)-(2.22), with $\epsilon \ll 1$ and $\beta \gg 1$, it is anticipated that a physically interesting, auto-conversion-related case entails the following quantitative relation between the values of the (more generally, independent) parameters ϵ, β :

$$\epsilon \equiv \frac{\beta^2}{2Le^2} \exp(-\beta T_\epsilon), \text{ with } T_\epsilon = 0(1). \quad (C.1)$$

It is convenient to introduce the notation

$$\begin{aligned} \bar{H}_\epsilon &\equiv (1 + T_\epsilon)^{-1} < 1 \Rightarrow T_\epsilon = (1 - \bar{H}_\epsilon) / \bar{H}_\epsilon; \\ \beta_\epsilon &= (1 + T_\epsilon) \beta > \beta. \end{aligned} \quad (C.2)$$

Hence, from (C.1) and (C.2),

$$\epsilon = \beta_\epsilon^2 \bar{H}_\epsilon^2 \exp(-\beta_\epsilon (1 - \bar{H}_\epsilon)) \quad (C.3)$$

The subscript ϵ denotes conditions at which it is anticipated that chemical conversion may no longer

be neglected in the end gas, although diffusive transfer remains negligible. This statement may be more readily noted by rewriting (2.16) and (2.17) under (C.1)-(C.3) as

$$\frac{\partial Y}{\partial t} \approx -\frac{1}{2Le^2} p Y (1 + \Phi Y) \exp\{-\beta_\epsilon (\bar{H}_\epsilon - T)/T\}, \quad (C.4)$$

$$\begin{aligned} \frac{\partial T}{\partial t} &\approx \frac{1}{2Le^2} p Y (1 + \Phi Y) \exp\{-\beta_\epsilon (\bar{H}_\epsilon - T)/T\} + \\ &\frac{\gamma - 1}{\gamma} \frac{(1 + KT)}{Kp} \frac{dp}{dt}. \end{aligned} \quad (C.5)$$

For $0 \leq T \leq \bar{H}_\epsilon$, the reaction term is negligible; this interval is also characterized by the following:

$$0 < t < \tau_\epsilon, \quad 1 < p < \Pi_\epsilon, \quad (C.6)$$

where the definitions of the constants τ_ϵ and Π_ϵ is evident. Within this interval, solution is given by (3.6a,b) in the unburned bulk gas, and by (3.9a,b) in the unburned end gas. For the typical values $\epsilon = 2 \times 10^{-4}$, $\beta \approx 10$, (c.1) gives $T_\epsilon \approx 1.31$, $\bar{H}_\epsilon \approx 0.432$, $\beta_\epsilon \approx 23.1$; for $\epsilon = 2 \times 10^{-4}$ but $\beta = 5$ (a somewhat small value), $T_\epsilon \approx 2.35$, $\bar{H}_\epsilon \approx 0.299$, $\beta_\epsilon \approx 16.8$. From (2.13), if $T_{00} \approx 300$ K, $T_{00} \approx 2100$ K, the condition $T = \bar{H}_\epsilon$ implies $T^* \approx 1078$ K for $\beta \approx 10$, $T^* \approx 840$ K for $\beta \approx 5$. The value for T^* used in the text is on the order of $\bar{H}_\epsilon \approx 0.4$, or $T^* \approx 1025$ K.

Equations (C.4) and (C.5) may be brought into the classical canonical form for study of transition to explosion by introduction of the following expansion about the state ϵ :

$$\tau = \beta_\epsilon \frac{(1 + \Phi)(\Pi_\epsilon / \bar{H}_\epsilon)}{2Le^2} (-\tau_\epsilon), \quad Y = 1 - \beta_\epsilon^{-1} \bar{H}_\epsilon X, \quad (C.7)$$

$$T = \bar{H}_\epsilon (1 + \beta_\epsilon^{-1} \bar{H}_\epsilon), \quad p = \Pi_\epsilon (1 + \beta_\epsilon^{-1} \Pi). \quad (C.8)$$

Substitution of (C.7) and (C.8) into (C.4) and (C.5) yields to leading order:

$$\begin{aligned} \frac{\partial X}{\partial \tau} &\approx \exp(\bar{H}_\epsilon), \quad \frac{\partial \Pi}{\partial \tau} \approx \exp(\bar{H}_\epsilon) + \\ &\frac{(\gamma - 1)}{\gamma} \frac{(1 + K \bar{H}_\epsilon)}{K \bar{H}_\epsilon} \frac{d\Pi}{d\tau}, \end{aligned} \quad (C.9a,b)$$

where

$$X = \bar{H}_\epsilon - \frac{(\gamma - 1)}{\gamma} \frac{(1 + K \bar{H}_\epsilon)}{K \bar{H}_\epsilon} \Pi \quad (C.10)$$

is an integral. To lowest order at the outset of the transition, reactant depletion need not be accounted for in the heat balance. Also, it is recalled that adjustment of the value of γ is taken as a convenient alternative to the introduction of a heat-transfer coefficient for incorporating thermal-loss effects during a process in which the pressure rises in time.^{§§}

^{§§} Compressional heating exceeds heat loss to walls in the end gas, for cases of automotive interest. Hence, the end gas is supercritical in the sense that pressure and temperature are assured to rise in time. The concern is whether or not the increase of temperature and pressure in time (from

Incidentally, from (C.1), (C.2), and (C.8), for a long-enough (say, adiabatic, constant-volume) duct, $\epsilon \rightarrow 0$, T_u increases and $(H)_u$ decreases; in such cases, chemical conversion could supplement significantly compression as a mechanism for unburned-gas preheating.

Acknowledgments

The authors are indebted to George Carrier of Harvard University for collaboration on earlier research in end-gas knock, and to Michal Dyer of Sandia Laboratories for urging the undertaking of this work. The authors are grateful to Ann McCollum for preparation of the manuscript and to Asenatha McCauley for preparation of the figures. Portions of this study were supported by the Army Research Office under contract DAAG29-83-C-0010 and by the Department of Energy under contract DE-AC04-78ET 13329.

References

- ¹Taylor, C. F., The Internal-Combustion Engine in Theory and Practice, Vol. 2, MIT Press, Cambridge, MA, 1968, pp. 34-85.
- ²Obert, E. F., Internal Combustion Engines and Air Pollution, Intext Educational Publishers, New York, NY, pp. 105-110, 291-341.
- ³Hirst, S. L., and Kirsch, L. J., "The Application of a hydrocarbon autoignition model in simulating knock and other engine combustion phenomena," Combustion Modeling in Reciprocating Engines, Plenum Press, New York, NY, pp. 193-229.
- ⁴Carrier, G. F., Fendell, F. E., Fink, S. F., and Feldman, P. S., "Heat transfer as a deterrent of end-gas knock," paper WSCI 83-30, April 1983 Meeting, Western States Section, Combustion Institute, Pasadena, CA.
- ⁵Carrier, G. F., Fendell, F. E., Bush, W. B., and Feldman, P. S., "Nonisenthalpic interaction of a planar premixed laminar flame with a parallel end wall," SAE Technical Paper 790245, Society of Automotive Engineers, Warrendale, PA, 1979.
- ⁶Fink, S. F., Fendell, F. E., and Bush, W. B., "Nonadiabatic nonisobaric propagation of a planar premixed flame: constant-volume enclosure," AIAA Paper 83-0239, 1983.
- ⁷Carrier, G. F., Fendell, F. E., and Feldman, P. S., "Nonisobaric flame propagation," Dynamics and Modeling of Reactive Systems, Academic Press, New York, NY, 1980, pp. 333-351.
- ⁸Senachin, P. K., and Babkin, V. S., "Self-ignition of gas in front of the flame front in a closed vessel," Fizika Goreniya i Vzryve, Vol. 18, No. 1, January-February 1982, pp. 3-8.
- ⁹Shivashinsky, G. I., "Hydrodynamic theory of flame propagation in an enclosed volume," Acta Astronautica, Vol. 6, 1979, pp. 631-645.
- ¹⁰Johnson, J. H., Myers, P. S., and Ueyehara, O. A., "End-gas temperature, pressures, reaction rates and knock," SAE Technical Paper 650505, Society of Automotive Engineers, Warrendale, PA, 1965.
- ¹¹Pitz, W. J., and Westbrook, C. K., "Chemical kinetics modeling of engine knock: preliminary results," paper WSCI 83-71, October 1983 Meeting, Western States Section, Combustion Institute, Los Angeles, CA.
- ¹²Guenoche, H., "Flame propagation in tubes and in closed vessels," Nonsteady Flame Propagation, Pergamon Press, Oxford, England, 1964, pp. 107-181.
- ¹³Steinert, W., Dunn-Rankin, D., and Sawyer, R. F., "Influence of chamber length and equivalence ratio on flame propagation in a constant-volume duct," Report LBL-14965, Energy and Environmental Division, Lawrence Berkeley Laboratory, Berkeley, CA, 1982.
- ¹⁴Egerton, A. C., Saunders, O. A., Lefebvre, A. H., and Moore, N. P. W., "Some observations by schlieren technique of the propagation of flames in a closed vessel," Fourth Symposium (International) on Combustion, Williams and Wilkins, Baltimore, MD, 1953, pp. 396-402.

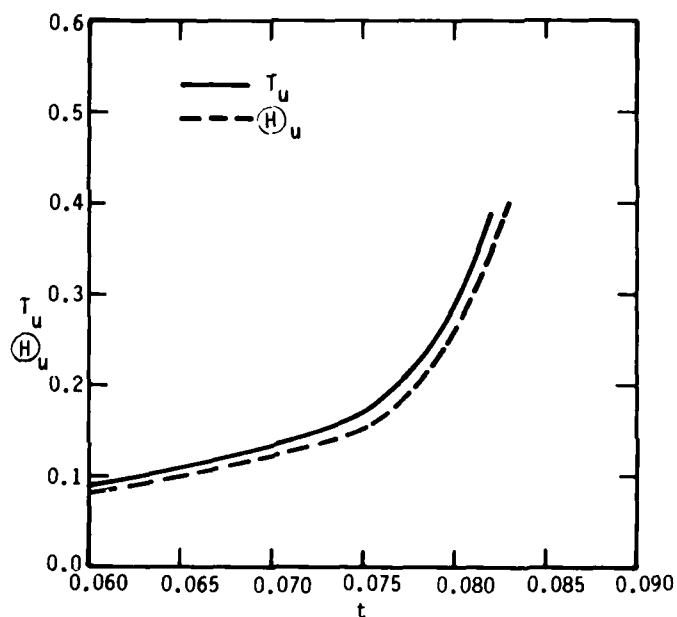


Fig. 1 For nominal parametric assignments, defined by (5.1)-(5.3), except that the compression ratio $CR=12$, the dimensionless unburned-bulk-gas temperature T_u and the dimensionless unburned-end-gas temperature $(H)_u$ are presented as functions of dimensionless time t , where compression commences at $t=0$. When the flame enters the end gas, T_u is no longer defined. Here, the scale for nondimensionalization of time is 22 ms; $T=0$ corresponds to 300 K, $T=0.2$, to 600 K, $T=0.4$ to 900 K. Augmented heat transfer from an appropriate portion of the mixture, the last-to-burn charge (end gas), precludes any unburned gas achieving a rapid-autoconversion-precipitating temperature, taken as 900 K.

the compressional-preheating/heat-loss balance) is such that transition to explosion is deferred so that completion of flame propagation occurs instead. Thus, while representing heat loss by adjustment of the polytropic constant precludes study of the near-critical state in which chemical exothermicity and heat loss balance, the present formulation is not aimed at such already well-studied questions.

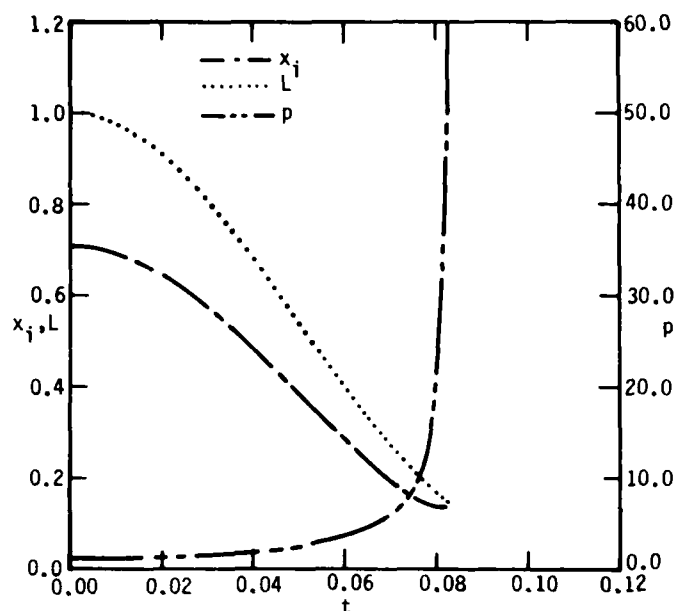


Fig. 2 For the case of Fig. 1, the dimensionless dependent variables pressure p , combustion-chamber length L , and interface position x_i between unburned bulk gas and unburned end gas are presented as functions of dimensionless time t . When the flame enters the end gas, x_i is no longer defined. Pressure is nondimensionalized against its initial value, here 1 atm, and lengths are nondimensionalized against the initial chamber length, here 10 cm.

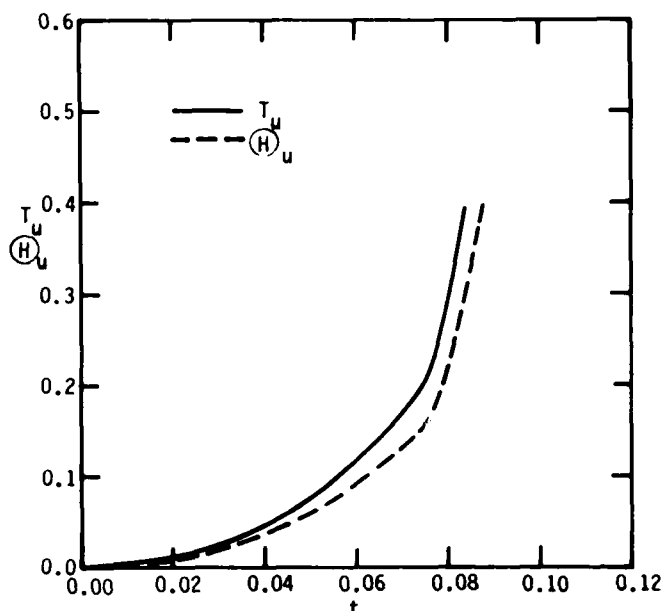


Fig. 4 For the nominal parametric assignments defined by (5.1)-(5.3), except that the ratio of chemical exothermicity to initial enthalpy $K = 3$, the dimensionless temperature T_u and the dimensionless unburned end-gas temperature $(H)_u$ are presented as functions of time t . The scale for nondimensionalization of time is 22 ms; $T = 0$ corresponds to 300 K, $T = 0.2$ to 620 K, $T = 0.4$ to 990 K (which is taken as the rapid-autoconversion-temperature to be avoided by augmented heat transfer from the end gas).

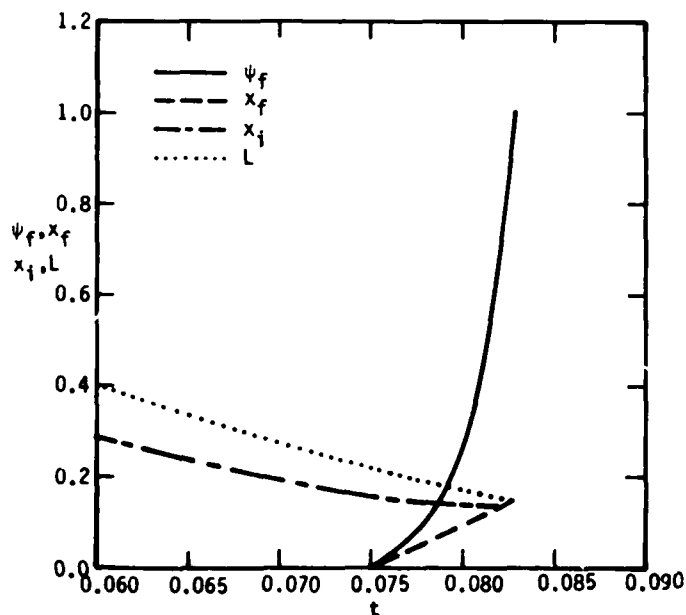


Fig. 3 For the case of Fig. 1, the dimensionless dependent variables chamber-length L , interface position x_i between unburned bulk gas and unburned end gas, the flame position x_f , and the fraction ψ_f of total initial premixture burned, are presented as functions of time t . The length x_f , like x_i , is nondimensionalized against initial chamber length, here 10 cm.

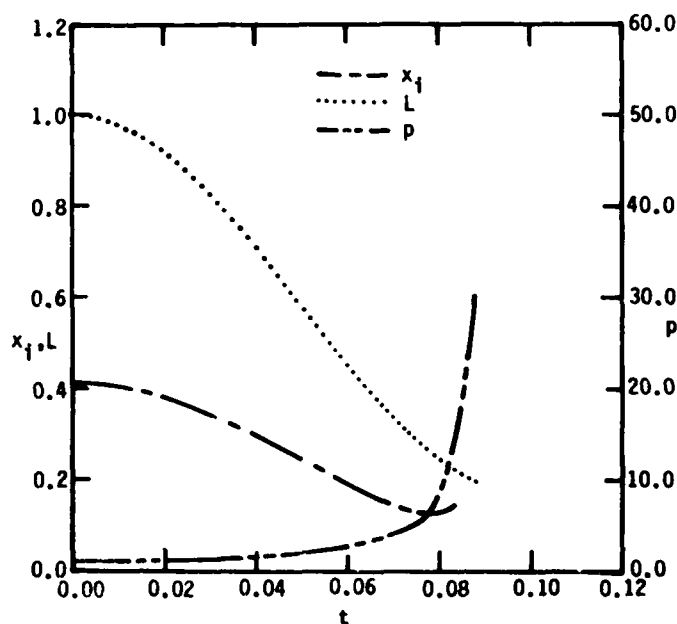


Fig. 5 For the case of Fig. 4, a presentation exactly analogous to that of Fig. 2.

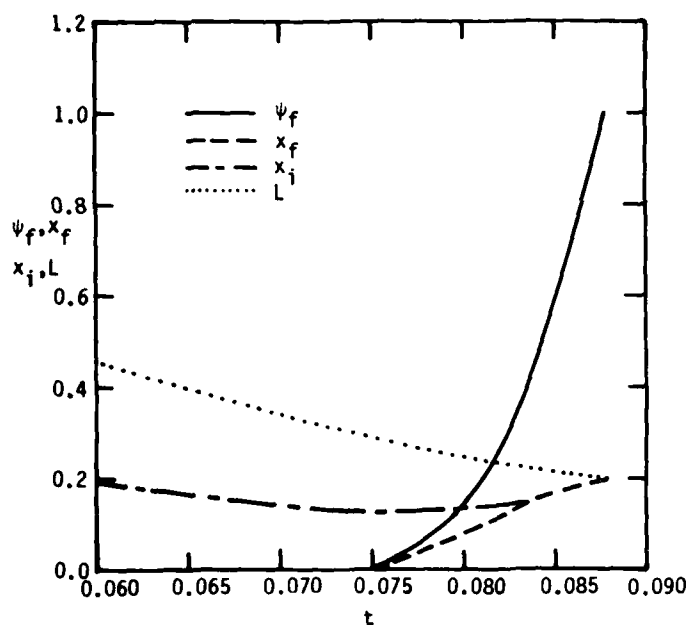


Fig. 6 For the case of Fig. 4, a presentation exactly analogous to that of Fig. 3.

Table 1. Parametric variations on the nominal (threshold-knock) case^a

Case	Flame enters end gas ($\psi_f = \psi_i$)							Flame propagation complete ($\psi_f = 1$)				
	\bar{t}	$\bar{\theta}^\circ$	\bar{L}	\bar{x}_f	$\bar{\psi}_f$	\bar{p}	\bar{H}_u	\bar{t}	$\bar{\theta}^\circ$	\bar{L}	\bar{p}	\bar{u}_{crit}
CR = 12	0.082	147.6	0.16	0.13	0.71	45.6	0.35	0.083	149.1	0.15	63.0	1.3604
K = 3	0.083	150.5	0.22	0.14	0.41	15.7	0.30	0.088	157.8	0.20	30.3	1.3002
$\omega = 51.6$	0.056	166.4	0.18	0.17	0.87	45.6	0.38	0.057	167.7	0.18	52.6	1.3836
$\theta_{ig} = 165^\circ$	0.098	77.0	0.17	0.16	0.83	46.2	0.37	0.099	177.9	0.17	54.3	1.3795

^aFor the case K = 3, if $p_0^* = 1$ atm, since $T_{u0}^* = 450$ K, then the initial density ρ_{u0}^* is reduced to two-thirds that of the other cases.

END

FILMED

4-84

DTIC